Biointerface Research in Applied Chemistry
Open-Access Journal (ISSN: 2069-5837)

Article
Volume 14, Issue 6, 2024, 140
https://doi.org/10.33263/BRIAC146.140

Exploring Marine Compounds for Inhibition of the BRAF V600E Mutation in Lung Cancer: A High Throughput Virtual Screening Approach

Anuj Singh [1], Krishna P Singh [2,*], Shailendra K Gupta [2,3], Deepak Ohri [1]

[1] Amity Institute of Biotechnology, Amity University Uttar Pradesh, Lucknow, (U.P), 226028, India; anuj.singh14@s.amity.edu(A.S); ohri_deepak@rediffmail.com(D.O.);
[2] Department of Systems Biology & Bioinformatics, University of Rostock, 18051, Rostock, Germany; krishna.singh@uni-rostock.de(K.P.S); shailendra.gupta@uni-rostock.de(S.G);
[3] Chhattisgarh Swami Vivekananda Technical University, 491107 Bhilai, India; shailendra.gupta@uni-rostock.de(S.G);
* Correspondence: krishna.singh@uni-rostock.de (K.P.S);

Scopus Author ID 59006392600
Received: 11.07.2023; Accepted: 28.01.2024; Published: 10.12.2024

Abstract: The BRAF V600E mutation is present in a variety of cancer cell types, including lung cancer, which is a leading cause of cancer-related death globally. Drugs like Dabrafenib and Vermaifenib were specifically used in targeted therapy for patients with BRAF V600E mutation. Drug resistance is typical, though, and more study is required to improve therapeutic strategies for this subset of lung cancer. Recently, marine natural compounds have emerged as a resource for the development of novel cancer therapeutics. In this study, we used virtual screening of marine compounds to find potential therapeutic candidates for NSCLC patients with the BRAF V600E mutation. We developed a receptor-based pharmacophore model and screened a library of 31,561 compounds from the Comprehensive Marine Natural Products Database (CMNPD) using a virtual screening protocol that was constructed and validated. Molecular docking was performed using CDOCKER to investigate potential inhibitors and ADMET for their toxicity and other properties. Seven compounds exhibited higher efficacy than the experimentally verified compound of BRAF mutation. A molecular dynamics simulation was performed to confirm the stability of the docked compounds and compare them with the experimentally verified compound. Our study identified, out of seven, the CMNPD7700 compound as a potential drug candidate for further development due to its high, effectiveness and molecular stability.

Keywords: lung cancer; BRAFV600E; high throughput virtual screening; marine natural compounds; receptor-based pharmacophore; molecular docking; molecular dynamics.

1. Introduction

Lung cancer is the most prevalent cancer in the world, accounting for about a quarter of deaths in all cancers. One of the lung cancers is Non-small cell lung cancer, contributing to 80–85% of all lung cancer cases. In India, 10.6% of the cancers were associated with lung cancer, containing both male and female patients [1]. In the present scenario, the major types of treatment that are available for the treatment of lung cancer are surgery, radiation therapy, chemotherapy,

and targeted therapies. Among these methods, targeted therapies demonstrated better outcomes during cancer treatment [2].

Various pathways are involved in the progression of lung cancer, like RAF–MEK–ERK pathway, PI3K signaling, JAK-STAT signaling, ERBB signaling pathway, etc., in which the RAS–RAF–MEK–ERK pathway plays a key role in malevolent cell progression in many tumors [3,4]. The BRAF (B-Raf proto-oncogene, serine/threonine kinase) gene encodes for a serine/threonine kinase that is part of the RAS-RAF-MEK-ERK axis that governs cellular development; mutations in BRAF are more common in current and past smokers as well as in with female and non-smokers compared to other oncogenic drivers [5–7]. Constitutive activation of the MAPK pathway is produced by B-Raf mutations, which makes cells more resistant to signals from the negative modulatory feedback loop and constantly stimulates their growth and proliferation. In actuality, B-Raf activating mutations are in charge of modifying the structural makeup of this protein, putting it into a persistently activated state and causing ongoing MEK and ERK activation [8]. In total, BARF cases in lung cancer over 90% of the reported BRAF-mutations V600E, corresponding to a Valine to Glutamate substitution at codon 600, with 10-fold higher basal kinase activity in comparison to wild-type (WT) BRAF [9–11].

Various targeted therapies are used to inhibit the effect of BRAF mutation; however, after initial success, these inhibitors start showing resistance and various side effects. An early-generation inhibitor, sorafenib, is being developed as a BRAF-specific targeted treatment. Although sorafenib's ability to inhibit MEK and ERK phosphorylation was suggested in preclinical models, clinical trials have not assessed the BRAF mutation status of the patients, so it is still unknown whether sorafenib can act as a BRAF inhibitor [12]. The next-generation inhibitors, dabrafenib, and vemurafenib, are specifically designed to suppress the BRAF V600E mutation. These inhibitors can be administered alone or in conjunction with existing inhibitors [13]. Compared to the commonly used inhibitors, these medications have significantly higher patient satisfaction and success rates. However, with time, these drugs cause drug resistance in most NSCLC patients, leading to a reactivation of the MAPK pathway, necessitating the employment of newer inhibitors development and combinations to solve these problems [14,15].

Since ancient times, natural compounds have been employed to cure various human ailments, from the discovery of penicillin to the most modern cancer-fighting medications like taxol, vinblastine, and camptothecin [16,17]. Over the past 50 years, emerging research has demonstrated that many natural substances derived from marine plants and microbes have beneficial effects in preventing and treating cancer. Examples include the marine-based medications cytarabine, eribulin mesylate, brentuximab vedotin, and trabectidine, which are used to treat leukemia, metastatic breast cancer, soft tissue sarcoma, and ovarian cancer [18–22].

For our study, we construct the receptor-based pharmacophore model based on the information taken from the published literature on the protein active site. Then, we validated our model with a set of active and inactive compounds. The model is used to screen the database of marine compounds to identify new potential hits for future drug design. Screened compounds are then subjected to molecular docking, based on which we gained higher docking scores of the 7 marine compounds compared to the experimentally taken known inhibitor. We also performed and ADMET analysis of these compounds. The MD simulations are performed to study the stability of docked compounds with the protein, which generally considers the conformational dynamics of

proteins for their stability in the system. These approaches are used to find new potential inhibitors with a comparable or higher binding orientation to already known ones. The steps of our study is shown in Figure 1.

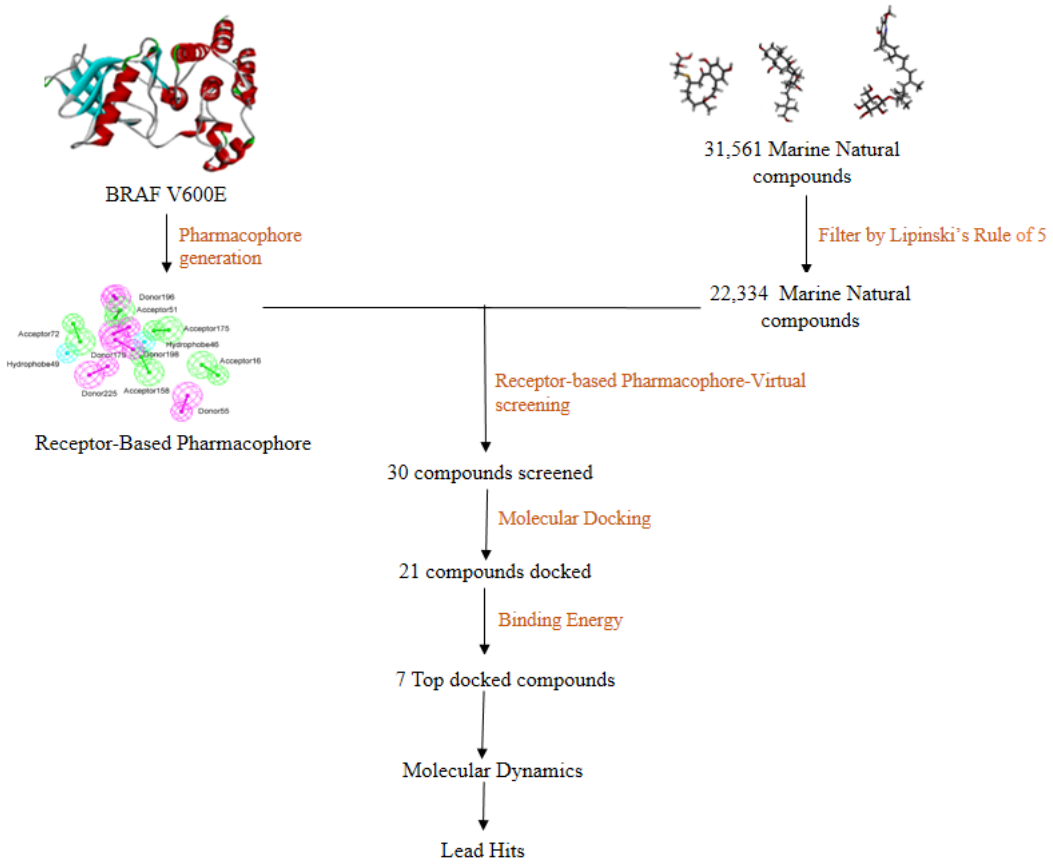

Figure 1. Diagrammatic representation of structure-based virtual screening protocol.

2. Materials and Methods

2.1. Three dimensional retrievals of protein.

The crystal structure of mutant BRAF V600E protein was retrieved from the protein data bank (PDB id:4XV2) [23]. The 'prepared protein' protocol of the Biovia Discovery Studio software suit (DS2022) was used to correct structure disorder, protein residue connectivity and bond orders, and missing side-chain or backbone atoms. The process of protein preparation mainly includes dehydration, double bond, and hydrogenation [24].

2.2. Selection and preparation of ligands.

We retrieved the compounds for the virtual screening from the Comprehensive Marine Natural Products Database (https://www.cmnpd.org/), a manually curated open-access knowledge repository devoted to marine natural product research. It offers details on 31,561 marine compound entities after duplicates were removed. It also includes the different physicochemical and pharmacokinetic properties, standardized biological activity data, systematic taxonomy, and the geographic distribution of source organisms [25]. These compounds were filtered using Lipinski's

rule of 5 to identify their drug-likeness and whether they had pharmacological features that would make them likely to be an oral treatment in humans [26,27]. The compounds filtered using Lipinski's rule of 5 are shown in Table S1.

2.3. Structure-based pharmacophore modeling.

We utilized the receptor-ligand interaction protocol present in DS 2022 to generate pharmacophores. The protein binding site was retrieved based on the protein-ligands interaction present in the active site cavity of the protein. Using the protocol 'receptor-ligands interaction', we identified common interacting residues of 10 experimentally verified compounds present in the active site cavity of the BRAF V600E [28–34]. Table S2 provides detailed information about the experimentally verified compounds, including their PubChem IDs and names. The active site pharmacophoric features were then identified using the 'Interaction Generation' protocol available in the DS2022. From the active site of BRAF V600E, we extracted the various pharmacophore features like hydrogen bond donors (HD), acceptors (HA), and hydrophobic (HY) pharmacophore features. We then optimized the features using the 'edit and cluster' protocol of the structure-based pharmacophore [35,36]. We have created the dataset of 10 previously experimentally verified compound inhibitors and 52 inactive compounds retrieved from Binding DB based on the IC50 value greater than 5nM. The dataset tests the discriminative ability of the generated receptor-based pharmacophore model to tell the difference between active and inactive compounds. The complete information on both active and inactive sets is provided in Table S3. The Gunner–Henry (GH) scoring method was used to measure the selectivity precision of hits and the recall of actives from a dataset of known actives and inactive [37]. This approach calculates total hits (Ht), % of actives yield, % of actives ratio, enrichment factor (E), false negatives, false positives, and goodness-of-hit score (GH). GH ranges from 0 to 1, representing null and ideal models [38].

2.4. Virtual screening.

Virtual screening has emerged as one of the most important methods for finding lead compounds for developing new medications. We used the protocol 'screen library' to screen the library of 22,335 compounds with the generated pharmacophore model. The minimum feature set in this was set to 4, the maximum feature set to 8, and the default values for all other parameters were left at their defaults. The input ligands conformation generation option was set to be the best in this instance [39].

2.5. Molecular docking.

Molecular docking was performed to understand the protein-compound interactions at the molecular level. We used the 'CDOCKER' docking protocol of DS2022, which is based on the CHARMm force field, and the receptor remains immobile while the compounds are permitted to flex. The CDOCKER energy, which represents ligand binding affinity, is computed for every complex conformation [40–42]. For docking, we selected the active site of the target protein BRAF V600E, which was the same site used in the structure-based pharmacophore modeling. The virtually screened natural compounds, the 10 experimentally verified inhibitor compounds, were

utilized and docked into the binding pocket of the target protein. Based on CDOCKER energy, many poses for each molecule were produced and examined.

2.6. ADMET analysis.

ADMET is a chemical's absorption, distribution, metabolism, excretion, and toxicity in an organism, estimated using the 'ADMET' protocol in the DS 2022. Six mathematical models were used to predict the ADMET properties of the compounds based on a set of rules. These models included aqueous solubility, blood-brain barrier penetration, CYP2D6 inhibition, hepatotoxicity, human intestinal absorption, and plasma protein binding. After performing molecular docking, we subjected only those ligands with higher CDOCKER energy than the experimentally verified inhibitor compounds to ADMET analysis. Compounds with high molecular docking energies were prioritized for this analysis.[43,44].

2.7. Molecular dynamics of the docked complexes.

To explore the stability of the docked complexes and understand the molecular interaction pattern of the compounds, we performed the Molecular Dynamics simulation by using the module 'Standard Dynamics Cascade' in the DS 2022. The compounds were subjected to MD simulation, which has higher docked energy than the experimentally verified inhibitor. For the MD simulations, the best docking poses for the target proteins-inhibitor complexes were selected based on their optimal binding conformations[45,46]. The system was exposed to the CHARMm force field and then relaxed by energy minimization (1000 steps of steepest descent and 1000 steps of conjugated gradient), with a final RMS gradient of 0.08326. A simulation of equilibration was run for 1 ns as the system was gradually heated from its beginning temperature of 50 K to the target temperature of 300 K. A time step of 2 fs was used for the MD simulations (production), which lasted for 10 ns which generate 5000 conformations against RMSD which is represented by A. The simulation was run under a constant volume, constant temperature (NVT) condition with a constant temperature of 300 K, and the data were stored at a frequency of 0.02 ns. Utilizing the analyze trajectory protocol DS 2022, the structural characteristics, root mean square deviation (RMSD), and potential energy of the MD trajectory were calculated. It is a commonly used measure of structural stability of the complex [47].

3. Results and Discussion

The receptor-based pharmacophore was generated using structural information from the BRAF V600E crystal structure. In the first step, we explore the receptor-ligand interaction of 10 experimentally verified compounds within the active site in order to identify the potentially important amino acids that make a strategic contribution to ligand binding. These amino acid residues were considered for the generation of pharmacophore. To create the pharmacophore model, we selected the most frequent occurring residues in the experimentally verified inhibitors sets, as shown in Table S2. The most frequent residue, such as CYS532, creates both hydrogen and hydrophobic bonds. The residues PHE583, TRP531, ALA481, LYS483, and LEU514, which form hydrophobic bonds with their respective experimentally verified inhibitors, were considered. In the second step, a sphere was created around the active site residue of BRAF V600E, using the

protocal ‘defining and editing’ binding sites present in DS 2022. By using the ‘Interaction Generation’ protocol, 757 features were generated: 204 acceptors (green), 413 donors (purple), and 140 hydrophobes (blue). For the selection of the features the tree graph clustering method was used to select the best feature elements. Clustering is based on the principle of distance matrix function to retain representative feature elements. The characteristic features matching the active residues of the BRAF V600E were selected manually. After that, 12 features (5 Acceptors, 5 Donors, and 2 Hydrophobes) were selected, as shown in Figure 2.

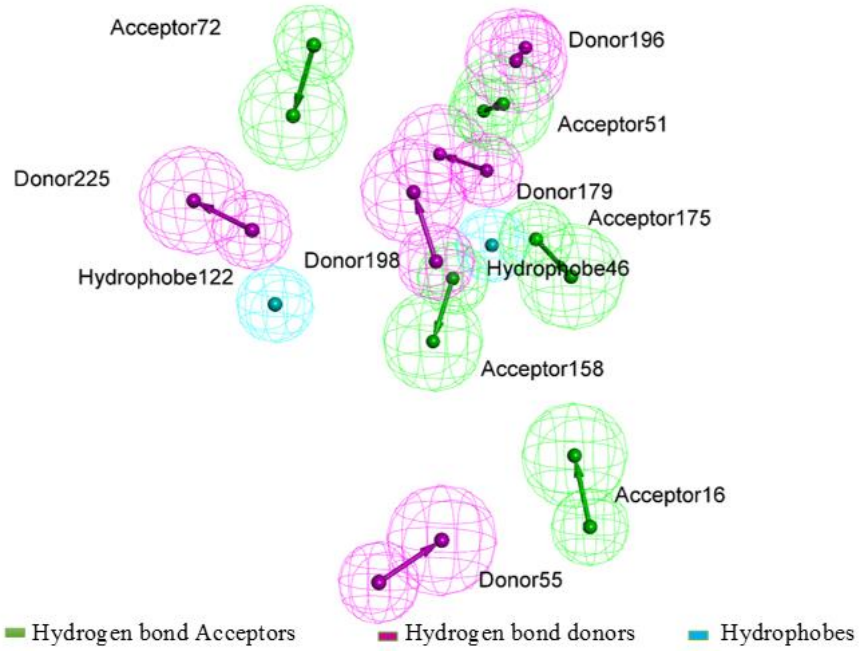

Figure 2. Selected structure-based pharmacophore features include hydrogen bond acceptor, doner, and hydrophobes.

The pharmacophore model was validated using a testing set of compounds containing 10 experimentally verified inhibitor compounds and 52 inactive compounds selected based on their IC50 values. The pharmacophore model was employed as a 3D query to carry out a virtual database search to verify the model's capacity to distinguish between active and inactive compounds; the results are given in Table 1. We selected the model with an E value of 48; after that, the model successfully identified 7 active compounds hits and 3 inactive compounds out of 10 screened, indicating its strong ability to distinguish between active and inactive. We also considered the second scoring function for the model; a GH score of 0.7-0.8 is considered excellent, and the pharmacophore model in this study had a GH score of 0.72, suggesting its efficiency for database screening based on validated results.

Table 1. Pharmacophore model validation using the goodness-of-hit score (GH) score method.

Serial No.	Parameter	Pharmacophore Model
1	Total molecules in database (*D*)	62
2	Total number of actives in the database (*A*)	10
3	Total hits (Ht)	9
4	Active hits (*Ha*)	7
5	% Yield of actives[(*Ha*/*Ht*) × 100]	77%

Serial No.	Parameter	Pharmacophore Model
6	% Ratio of actives [(*Ha*/*A*) × 100]	70%
7	Enrichment factor (*E*) [(*Ha* × *D*)/(*Ht* × *A*)]	48
8	False negatives [*A* − *Ha*]	3
9	False positives [*Ht* − *Ha*]	2
10	Goodness of hit score (*GH*) *	0.72

After the model validation based on the active and inactive, we considered 22,335 marine compunds that had already passed Lipinski's rule of 5 for their durability and selected for the virtual screening against the receptor-based pharmacophore using a 'screen library' protocol of DS 2022. All the 22,335 marine compounds were screened with a receptor-based pharmacophore model with pharmacophoric features larger than or equal to 4 but less than or equal to 8. A total of 30 compounds (Table S4) were screened in the process, and some of them were as shown in Figure 3.

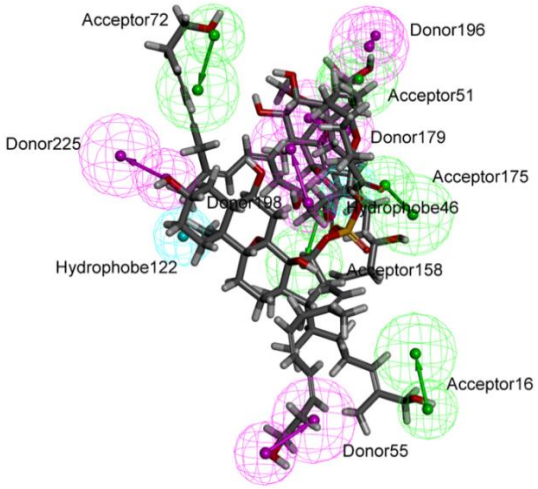

Figure 3. Virtual screening of marine compounds based on the pharmacophoric features and some of the few compounds were shown in the figure.

The 'CDOCKER' protocol was utilized for the molecular docking analysis of 30 ligands selected through virtual screening, along with the 10 experimentally verified BRAF V600E inhibitors. Of the 30 natural compounds, 21 were able to dock into the BRAF V600E protein, and 10 experimentally verified inhibitors were successfully docked as well. Notably, seven of the screened compounds exhibited higher docking energies than any of the known experimentally verified inhibitors, as detailed in Table 2 with their respective CDOCKER Energy values (kcal/mol).

Table 2. CDOCKER Energy of top 7 natural compounds along with an experimentally verified inhibitor.

S.No.	Compounds	PubChem ID	CDOCKER Energy (kcal/mol)
1	CMNPD7700	15167968	-906.269
2	CMNPD4630	163006495	-799.895
3	CMNPD7209	163145067	-775.943
4	CMNPD10093	162842689	-645.889
5	CMNPD1425	23425463	-442.052
6	CMNPD29590	145951601	-417.776
7	CMNPD31300	163110523	-369.563
8	Dabrafenib	44462760	-189.491

We further investigated the interaction of the compounds with the amino acid residues present in the protein active site. The highest energy marine natural compound (CMNPD7700) formed a hydrogen bond with LYS483, ASP594, SER605, GLY606, SER607, while hydrophobic bonds with ILE463, VAL471, ALA481, LEU514, TRP531, PHE583 while experimentally verified compound (Dabrafenib) forms hydrogen Bond with ASP594 and hydrophobic bonds with VAL471, ALA481, LEU514, CYS532, PHE583, GLY606, SER607. The CDOCKER energy of the 21 natural compounds and 10 experimentally verified docked compounds are given in Table S5, and the bond information of top 2 compounds (CMNPD7700 and Dabrafenib)from both the lists are given in Table S6.

The ADMET module of DS2022 was employed to predict the therapeutic properties of top-docked compounds as well as the experimentally verified docked compounds,. The ADMET properties, including aqueous solubility, blood-brain barrier level, CYP2D6 binding, hepatotoxicity, human intestinal absorption level, and plasma protein binding properties, are shown in Table 3. Our analysis revealed that CMNPD1425, CMNPD29590, and CMNPD4630 passed all the criteria of ADMET properties, whereas compounds CMNPD7209, CMNPD31300, and CMNPD10093 exhibited low absorption according to criteria and CMNPD7700 is Hepatotoxic in comparison to the experiment compound show low solubility, absorption and also toxic properties.

Table 3. Predicted ADMET properties of the top 7 marine natural compounds along with top experimentally verified compounds.

S.No.	Compound Name	PubChem ID	Solubility level	BBB level	CYP2 D6	Hepatotoxicity	Absorption level	PPB level
1	CMNPD7700	15167968	3 (good)	4 (very low)	FALSE	TRUE	1 (moderate)	FALSE (Binding is >90%)
2	CMNPD4630	163006495	4 (optimal)	4 (very low)	FALSE	FALSE	0 (good)	TRUE (Binding is <90%)
3	CMNPD7209	163145067	3 (good)	4 (very low)	FALSE	FALSE	3 (very poor)	TRUE (Binding is <90%)
4	CMNPD10093	162842689	3 (good)	4 (very low)	FALSE	FALSE	2 (poor)	TRUE (Binding is <90%)
5	CMNPD1425	23425463	3 (good)	3 (Low)	FALSE	FALSE	0 (good)	TRUE (Binding is <90%)
6	CMNPD29590	145951601	3 (good)	4 (very low)	FALSE	FALSE	0 (good)	TRUE (Binding is <90%)
7	CMNPD31300	163110523	3 (good)	3 (Low)	FALSE	FALSE	0 (good)	TRUE (Binding is <90%)
8	Dabrafenib	44462760	0 (extremely low)	4 (very low)	FALSE	TRUE	2 (poor)	TRUE (Binding is <90%)

To assess the stability of the the protein-compound complexes of the lead compounds, we conducted a 10 ns of molecular dynamic simulation using the DS2022. The resulting trajectory files obtained from the simulation were analyzed based on the RMSD; protein-ligand interaction, intra-molecular hydrogen, and hydrophobic bonds were evaluated. These analyses demonstrated

the stability of our 7 lead compounds compared to the experimentally verified inhibitor. Our results indicated that all docked compounds reached convergence within this timeframe, as illustrated in RMSD Figure 4.

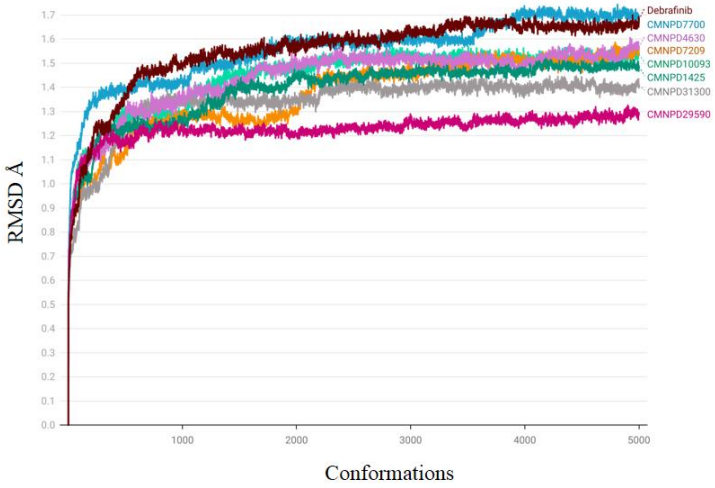

Figure 4. The root-mean-square deviation (RMSD) of the top 7 inhibitors and the reference compounds.

To analyze the dynamics result, we examined the hydrogen interaction and hydrophobic by evaluating the number of bond formations at the start of the simulation and after the 10 ns production run. Table 4 presents the comparison of bond formations following molecular docking with those observed in the last frame of the dynamics simulation.

Table 4. The number of hydrogen bonds and hydrophobic bonds forms in molecular docking and molecular dynamics.

S.No.	Compound Name	Molecular Docking		Molecular Dynamics Stimulation	
		No. of Hydrogen Bond	No. of Hydrophobic Bond	No. of Hydrogen Bond	No. of Hydrophobic Bond
1	CMNPD7700	7	9	12	13
2	CMNPD4630	3	9	5	9
3	CMNPD7209	5	8	5	6
4	CMNPD10093	9	10	5	5
5	CMNPD1425	6	10	6	11
6	CMNPD29590	3	13	2	10
7	CMNPD31300	4	6	2	9
8	Dabrafenib	2	9	3	5

The MD simulation analysis revealed that the compound that has the highest CDOCKER energy (CMNPD7700) earlier formed 7 Hydrogen bonds and 9 Hydrophobic bonds with various residues. After the 10 ns of the production run, the number of bonds formed increased to 12 Hydrogen bond and 13 hydrophobic bonds. The compound not only retained the earlier formed Hydrogen bonds with LYS483, ASP594, SER605, GLY606, and SER607 but also formed new bonds with ILE592, GLY593, and PHE595 while it retained Hydrophobic bonds ILE463, ALA481, LEU514, PHE583 and while forming new bonds with TRP531 and CYS532, losing only the bond with VAL471.. This suggests a higher stability of the complex, In contrast, the inhibitor dabrafenib, which initially formed 2 hydrogen bonds and 9 hydrophobic bonds, only gained 1

additional hydrogen bond with CYS532 and SER607 after the simulation while retaining the bond with ASP594. However, it lost 4 hydrophobic bonds, retaining interactions with only ALA481, LEU514, PHE583, and GLY606 and losing those with CYS532 and VAL471. This indicates lower stability of the dabrafenib complex compared to the natural compound CMNPD7700.

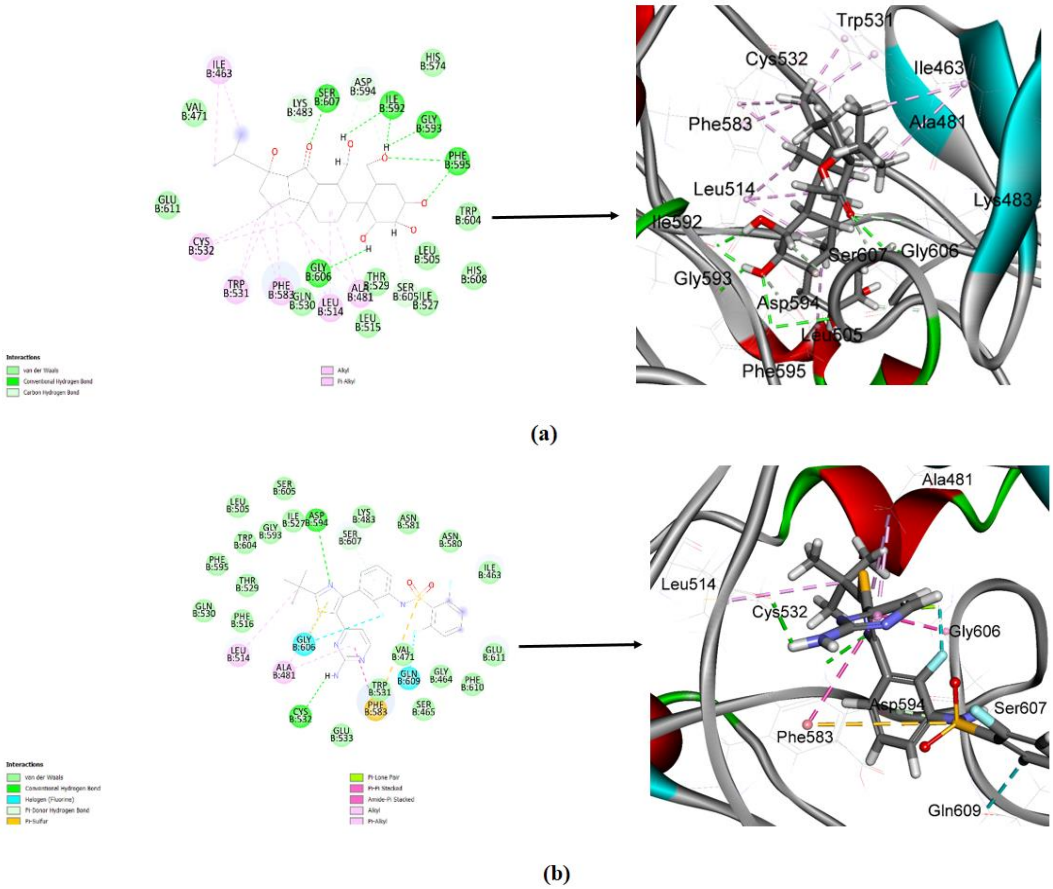

Figure 5. Interaction between BRAF V600E and ligands (a) CMNPD7700; (b) Dabrafenib showing 2D and 3D interaction representations are shown in the left and right panels, respectively.

The bond form during the last frame for both the CMNPD7700-BRAF V600E complex (Figure 5a) and dabrafenib-BRAF V600E complex (Figure 5b) is shown respectively. The detailed bond information formed after the last frame of the two compounds is given in Table S7.

4. Conclusion

The goal of the current research was to identify novel natural inhibitors for the BRAF V600E mutant, a critical target for a number of cancer-related issues, most notably lung cancer and melanoma. We create a structure-based pharmacophore model after understanding the essential structural characteristics of the active site from the experimentally verified inhibitor. This model, which was modified and constructed around the active site, aids in the identification of crucial components needed for an inhibitor. 22,334 drug-like compounds were extracted from the 31,561 marine natural compound library after filtering them through Lipinski's Rule of 5 and chosen for virtual screening using the pharmacophore model; after being evaluated for their features, 30 natural compounds were screened. Following molecular docking and ADMET

analysis on these screened compounds, seven compounds, CMNPD7700, CMNPD4630, CMNPD7209, CMNPD10093, CMNPD1425, CMNPD29590, and CMNPD31300, with the highest molecular docking scores against known inhibitors are chosen. These docked compounds are then studied for their stability through molecular dynamics for 10 ns.After this we found that the top natural marine compound (CMNPD7700), which has the highest docking energy, is more stable and formed the more interction with the residues of BRAF V600E compared to the experimentally verified compounds. Therefore, our studies provide strong evidence that these compounds may be novel lead compounds as inhibitor drug candidates. Overall, our study provides new insights into the potential anticancer activity of marine compounds against lung cancer targets. Our findings highlight the importance of natural compounds in drug discovery and molecular docking in identifying novel anticancer agents. Further experimental studies are needed to validate the therapeutic potential of these natural compounds and their safety profile in developing lead inhibitors.

Funding

This research was funded by the German Federal Ministry of Education and Research (BMBF) e: Med-MelAutim 01ZX2205B to S.G. and K.P.S.

Conflict of interest

The authors declare that they have no competing or conflicts of interest.

Acknowledgments

We thank Olaf Wolkenhauer for the logistics and continued support.

Conflict of Interest

The authors declare that they have no competing or conflicts of interest.

References

1. Kulothungan, V.; Sathishkumar, K.; Leburu, S.; Ramamoorthy, T.; Stephen, S.; Basavarajappa, D.; Tomy, N.; Mohan, R.; Menon, G.R.; Mathur, P. Burden of cancers in India - estimates of cancer crude incidence, YLLs, YLDs and DALYs for 2021 and 2025 based on National Cancer Registry Program. *BMC Cancer* **2022**, *22*, 527, https://doi.org/10.1186/s12885-022-09578-1.
2. Yuan, M.; Huang, L.-L.; Chen, J.-H.; Wu, J.; Xu, Q. The emerging treatment landscape of targeted therapy in non-small-cell lung cancer. *Signal Transduct. Target. Ther.* **2019**, *4*, 61, https://doi.org/10.1038/s41392-019-0099-9.
3. Chrysanthakopoulos, N.A.; Dareioti, N.S. Molecular abnormalities and cellular signaling pathways alterations in lung cancer. *Med. Dent. Res.* **2018**, *1*, https://doi.org/10.15761/mdr.1000105.
4. Thirunavukkarasu, M.K.; Suriya, U.; Rungrotmongkol, T.; Karuppasamy, R. In Silico Screening of Available Drugs Targeting Non-Small Cell Lung Cancer Targets: A Drug Repurposing Approach. *Pharmaceutics* **2022**, *14*, 59, https://doi.org/10.3390/pharmaceutics14010059.
5. Villaruz, L.C.; Socinski, M.A.; Abberbock, S.; Berry, L.D.; Johnson, B.E.; Kwiatkowski, D.J.; Iafrate, A.J.; Varella-Garcia, M.; Franklin, W.A.; Camidge, D.R.; Sequist, L.V.; Haura, E.B.; Ladanyi, M.; Kurland, B.F.; Kugler, K.; Minna, J.D.; Bunn, P.A.; Kris, M.G. Clinicopathologic features and outcomes of patients with lung adenocarcinomas harboring *BRAF* mutations in the Lung Cancer Mutation Consortium. *Cancer* **2015**, *121*, 448–

456, https://doi.org/10.1002/cncr.29042.
6. Tissot, C.; Couraud, S.; Tanguy, R.; Bringuier, P.-P.; Girard, N.; Souquet, P.-J. Clinical characteristics and outcome of patients with lung cancer harboring BRAF mutations. *Lung Cancer* **2016**, *91*, 23–28, https://doi.org/10.1016/j.lungcan.2015.11.006.
7. Cui, G.; Liu, D.; Li, W.; Fu, X.; Liang, Y.; Li, Y.; Shi, W.; Chen, X.; Zhao, S. A meta-analysis of the association between BRAF mutation and non-small cell lung cancer. *Medicine* **2017**, *96*, e6552, https://doi.org/10.1097/MD.0000000000006552.
8. Caparica, R.; de Castro, G.; Gil-Bazo, I.; Caglevic, C.; Calogero, R.; Giallombardo, M.; Santos, E.S.; Raez, L.E.; Rolfo, C. BRAF mutations in non-small cell lung cancer: has finally Janus opened the door?. *Crit. Rev. Oncol. Hematol.* **2016**, *101*, 32–39, https://doi.org/10.1016/j.critrevonc.2016.02.012.
9. Luo, C.; Xie, P.; Marmorstein, R. Identification of BRAF Inhibitors through In Silico Screening. *J. Med. Chem.* **2008**, *51*, 6121–6127, https://doi.org/10.1021/jm800539g.
10. Marchetti, A.; Felicioni, L.; Malatesta, S.; Sciarrotta, M.G.; Guetti, L.; Chella, A.; Viola, P.; Pullara, C.; Mucilli, F.; Buttitta, F. Clinical Features and Outcome of Patients with Non-Small-Cell Lung Cancer Harboring *BRAF* Mutations. *J. Clin. Oncol.* **2011**, *29*, 3574–3579, https://doi.org/10.1200/JCO.2011.35.9638.
11. Roviello, G.; D'Angelo, A.; Sirico, M.; Pittacolo, M.; Conter, F.U.; Sobhani, N. Advances in anti-BRAF therapies for lung cancer. *Invest. New Drugs* **2021**, *39*, 879–890, https://doi.org/10.1007/s10637-021-01068-8.
12. Yan, N.; Guo, S.; Zhang, H.; Zhang, Z.; Shen, S.; Li, X. BRAF-Mutated Non-Small Cell Lung Cancer: Current Treatment Status and Future Perspective. *Front. Oncol.* **2022**, *12*, 863043, https://doi.org/10.3389/fonc.2022.863043.
13. Subbiah, V.; Baik, C.; Kirkwood, J.M. Clinical Development of BRAF plus MEK Inhibitor Combinations. *Trends Cancer* **2020**, *6*, 797–810, https://doi.org/10.1016/j.trecan.2020.05.009.
14. Facchinetti, F.; Lacroix, L.; Mezquita, L.; Scoazec, J.-Y.; Loriot, Y.; Tselikas, L.; Gazzah, A.; Rouleau, E.; Adam, J.; Michiels, S.; Massard, C.; André, F.; Olaussen, K.A.; Vassal, G.; Howarth, K.; Besse, B.; Soria, J.-C.; Friboulet, L.; Planchard, D. Molecular mechanisms of resistance to BRAF and MEK inhibitors in $BRAF^{V600E}$ non–small cell lung cancer. *Eur. J. Cancer* **2020**, *132*, 211–223, https://doi.org/10.1016/j.ejca.2020.03.025.
15. Sforza, V.; Palumbo, G.; Cascetta, P.; Carillio, G.; Manzo, A.; Montanino, A.; Sandomenico, C.; Costanzo, R.; Esposito, G.; Laudato, F.; Damiano, S.; Forte, C.A.; Frosini, G.; Farese, S.; Piccirillo, M.C.; Pascarella, G.; Normanno, N.; Morabito, A. BRAF Inhibitors in Non-Small Cell Lung Cancer. *Cancers* **2022**, *14*, 4863, https://doi.org/10.3390/cancers14194863.
16. Cragg, G.M.; Pezzuto, J.M. Natural Products as a Vital Source for the Discovery of Cancer Chemotherapeutic and Chemopreventive Agents. *Med. Princ. Pract.* **2016**, *25*, 41–59, https://doi.org/10.1159/000443404.
17. Riaz, M.; Khalid, R.; Afzal, M.; Anjum, F.; Fatima, H.; Zia, S.; Rasool, G.; Egbuna, C.; Mtewa, A.G.; Uche, C.Z.; Aslam, M.A. Phytobioactive compounds as therapeutic agents for human diseases: A review. *Food Sci. Nutr.* **2023**, *11*, 2500–2529, https://doi.org/10.1002/FSN3.3308.
18. Khalifa, S.A.M.; Elias, N.; Farag, M.A.; Chen, L.; Saeed, A.; Hegazy, M.-E.F.; Moustafa, M.S.; Abd El-Wahed, A.; Al-Mousawi, S.M.; Musharraf, S.G.; Chang, F.-R.; Iwasaki, A.; Suenaga, K.; Alajlani, M.; Göransson, U.; El-Seedi, H.R. Marine Natural Products: A Source of Novel Anticancer Drugs. *Mar. Drugs* **2019**, *17*, 491, https://doi.org/10.3390/md17090491.
19. Sigwart, J.D.; Blasiak, R.; Jaspars, M.; Jouffray, J.-B.; Tasdemir, D. Unlocking the potential of marine biodiscovery. *Nat. Prod. Rep.* **2021**, *38*, 1235–1242, https://doi.org/10.1039/d0np00067a.
20. Kulkarni, A.M.; Kumar, V.; Parate, S.; Lee, G.; Yoon, S.; Lee, K.W. Identification of New KRAS G12D Inhibitors through Computer-Aided Drug Discovery Methods. *Int. J. Mol. Sci.* **2022**, *23*, 1309, https://doi.org/10.3390/ijms23031309.
21. Kumar, V.; Parate, S.; Yoon, S.; Lee, G.; Lee, K.W. Computational Simulations Identified Marine-Derived Natural Bioactive Compounds as Replication Inhibitors of SARS-CoV-2. *Front. Microbiol.* **2021**, *12*, 647295, https://doi.org/10.3389/fmicb.2021.647295.
22. Almaliti, J.; Gerwick, W.H. Methods in marine natural product drug discovery: what's new?. *Expert Opin. Drug Discov.* **2023**, *18*, 687–691, https://doi.org/10.1080/17460441.2023.2214360.
23. Zhang, C.; Spevak, W.; Zhang, Y.; Burton, E.A.; Ma, Y.; Habets, G.; Zhang, J.; Lin, J.; Ewing, T.; Matusow, B.; Tsang, G.; Marimuthu, A.; Cho, H.; Wu, G.; Wang, W.; Fong, D.; Nguyen, H.; Shi, S.; Womack, P.; Nespi, M.;

Shellooe, R.; Carias, H.; Powell, B.; Light, E.; Sanftner, L.; Walters, J.; Tsai, J.; West, B.L.; Visor, G.; Rezaei, H.; Lin, P.S.; Nolop, K.; Ibrahim, P.N.; Hirth, P.; Bollag, G. RAF inhibitors that evade paradoxical MAPK pathway activation. *Nature* **2015**, *526*, 583–586, https://doi.org/10.1038/nature14982.

24. Zheng, S.-L.; Luo, Q.-B.; Suo, S.-K.; Zhao, Y.-Q.; Chi, C.-F.; Wang, B. Preparation, Identification, Molecular Docking Study and Protective Function on HUVECs of Novel ACE Inhibitory Peptides from Protein Hydrolysate of Skipjack Tuna Muscle. *Mar. Drugs* **2022**, *20*, 176, https://doi.org/10.3390/MD20030176.
25. Lyu, C.; Chen, T.; Qiang, B.; Liu, N.; Wang, H.; Zhang, L.; Liu, Z. CMNPD: a comprehensive marine natural products database towards facilitating drug discovery from the ocean. *Nucleic Acids Res.* **2021**, *49*, D509–D515, https://doi.org/10.1093/nar/gkaa763.
26. Lipinski, C.A. Lead- and drug-like compounds: the rule-of-five revolution. *Drug Discov. Today Technol.* **2004**, *1*, 337–341, https://doi.org/10.1016/j.ddtec.2004.11.007.
27. Belal, A.; Elkady, H.; Al-Karmalawy, A.A.; Amin, A.H.; Ghoneim, M.M.; El-Sherbiny, M.; Al-Serwi, R.H.; Abdou, M.A.; Ibrahim, M.H.; Mehany, A.B.M. Discovery of Some Heterocyclic Molecules as Bone Morphogenetic Protein 2 (BMP-2)-Inducible Kinase Inhibitors: Virtual Screening, ADME Properties, and Molecular Docking Simulations. *Molecules* **2022**, *27*, 5571, https://doi.org/10.3390/MOLECULES27175571.
28. Bollag, G.; Hirth, P.; Tsai, J.; Zhang, J.; Ibrahim, P.N.; Cho, H.; Spevak, W.; Zhang, C.; Zhang, Y.; Habets, G.; Burton, E.A.; Wong, B.; Tsang, G.; West, B.L.; Powell, B.; Shellooe, R.; Marimuthu, A.; Nguyen, H.; Zhang, K.Y.J.; Artis, D.R.; Schlessinger, J.; Su, F.; Higgins, B.; Iyer, R.; D'Andrea, K.; Koehler, A.; Stumm, M.; Lin, P.S.; Lee, R.J.; Grippo, J.; Puzanov, I.; Kim, K.B.; Ribas, A.; McArthur, G.A.; Sosman, J.A.; Chapman, P.B.; Flaherty, K.T.; Xu, X.; Nathanson, K.L.; Nolop, K. Clinical efficacy of a RAF inhibitor needs broad target blockade in *BRAF*-mutant melanoma. *Nature* **2010**, *467*, 596–599, https://doi.org/10.1038/NATURE09454.
29. Tang, Z.; Yuan, X.; Du, R.; Cheung, S.-H.; Zhang, G.; Wei, J.; Zhao, Y.; Feng, Y.; Peng, H.; Zhang, Y.; Du, Y.; Hu, X.; Gong, W.; Liu, Y.; Gao, Y.; Liu, Y.; Hao, R.; Li, S.; Wang, S.; Ji, J.; Zhang, L.; Li, S.; Sutton, D.; Wei, M.; Zhou, C.; Wang, L.; Luo, L. BGB-283, a Novel RAF Kinase and EGFR Inhibitor, Displays Potent Antitumor Activity in *BRAF*-Mutated Colorectal Cancers. *Mol. Cancer Ther.* **2015**, *14*, 2187–2197, https://doi.org/10.1158/1535-7163.MCT-15-0262.
30. Tsai, J.; Lee, J.T.; Wang, W.; Zhang, J.; Cho, H.; Mamo, S.; Bremer, R.; Gillette, S.; Kong, J.; Haass, N.K.; Sproesser, K.; Li, L.; Smalley, K.S.M.; Fong, D.; Zhu, Y.-L.; Marimuthu, A.; Nguyen, H.; Lam, B.; Liu, J.; Cheung, I.; Rice, J.; Suzuki, Y.; Luu, C.; Settachatgul, C.; Shellooe, R.; Cantwell, J.; Kim, S.-H.; Schlessinger, J.; Zhang, K.Y.J.; West, B.L.; Powell, B.; Habets, G.; Zhang, C.; Ibrahim, P.N.; Hirth, P.; Artis, D.R.; Herlyn, M.; Bollag, G. Discovery of a selective inhibitor of oncogenic B-Raf kinase with potent antimelanoma activity. *Proc. Natl. Acad. Sci. U.S.A.* **2008**, *105*, 3041–3046, https://doi.org/10.1073/PNAS.0711741105.
31. Wenglowsky, S.; Moreno, D.; Laird, E.R.; Gloor, S.L.; Ren, L.; Risom, T.; Rudolph, J.; Sturgis, H.L.; Voegtli, W.C. Pyrazolopyridine inhibitors of B-Raf^{V600E}. Part 4: Rational design and kinase selectivity profile of cell potent type II inhibitors. *Bioorg. Med. Chem. Lett.* **2012**, *22*, 6237–6241, https://doi.org/10.1016/J.BMCL.2012.08.007.
32. Haling, J.R.; Sudhamsu, J.; Yen, I.; Sideris, S.; Sandoval, W.; Phung, W.; Bravo, Brandon J.; Giannetti, Anthony M.; Peck, A.; Masselot, A.; Morales, T.; Smith, D.; Brandhuber, B.J.; Hymowitz, S.G.; Malek, S. Structure of the BRAF-MEK Complex Reveals a Kinase Activity Independent Role for BRAF in MAPK Signaling. *Cancer Cell* **2014**, *26*, 402–413, https://doi.org/10.1016/J.CCR.2014.07.007.
33. Cotto-Rios, X.M.; Agianian, B.; Gitego, N.; Zacharioudakis, E.; Giricz, O.; Wu, Y.; Zou, Y.; Verma, A.; Poulikakos, P.I.; Gavathiotis, E. Inhibitors of BRAF dimers using an allosteric site. *Nat. Commun.* **2020**, *11*, 4370, https://doi.org/10.1038/S41467-020-18123-2.
34. Luo, L.; Zhong, A.; Wang, Q.; Zheng, T. Structure-Based Pharmacophore Modeling, Virtual Screening, Molecular Docking, ADMET, and Molecular Dynamics (MD) Simulation of Potential Inhibitors of PD-L1 from the Library of Marine Natural Products. *Mar. Drugs* **2022**, *20*, 29, https://doi.org/10.3390/MD20010029.
35. Ma, Y.-C.; Yang, B.; Wang, X.; Zhou, L.; Li, W.-Y.; Liu, W.-S.; Lu, X.-H.; Zheng, Z.-H.; Ma, Y.; Wang, R.-L. Identification of novel inhibitor of protein tyrosine phosphatases delta: structure-based pharmacophore modeling, virtual screening, flexible docking, molecular dynamics simulation, and post-molecular dynamics analysis. *J. Biomol. Struct. Dyn.* **2020**, *38*, 4432–4448, https://doi.org/10.1080/07391102.2019.1682050.
36. Szwabowski, G.L.; Daigle Jr., B.J.; Baker, D.L.; Parrill, A.L. Structure-based pharmacophore modeling 2. Developing a novel framework for structure-based pharmacophore model generation and selection. *J. Mol.*

Graph. Model. **2023**, *122*, 108488, https://doi.org/10.1016/J.JMGM.2023.108488.
37. Zhou, Y.; Di, B.; Niu, M.-M. Structure-Based Pharmacophore Design and Virtual Screening for Novel Tubulin Inhibitors with Potential Anticancer Activity. *Molecules* **2019**, *24*, 3181, https://doi.org/10.3390/molecules24173181.
38. Ghosh, A.; Mukherjee, S.; Jha, P.C.; Manhas, A. Identifying natural product inhibitors against CDK9 enzyme via combined multicomplex-based pharmacophore modeling, interaction studies and molecular dynamics simulations. *Comput. Biol. Med.* **2023**, *161*, 107055, https://doi.org/10.1016/J.COMPBIOMED.2023.107055.
39. Fu, Y.; Sun, Y.-N.; Yi, K.-H.; Li, M.-Q.; Cao, H.-F.; Li, J.-Z.; Ye, F. 3D Pharmacophore-Based Virtual Screening and Docking Approaches toward the Discovery of Novel HPPD Inhibitors. *Molecules* **2017**, *22*, 959, https://doi.org/10.3390/molecules22060959.
40. Gogoi, B.; Chowdhury, P.; Goswami, N.; Gogoi, N.; Naiya, T.; Chetia, P.; Mahanta, S.; Chetia, D.; Tanti, B.; Borah, P.; Handique, P.J. Identification of potential plant-based inhibitor against viral proteases of SARS-CoV-2 through molecular docking, MM-PBSA binding energy calculations and molecular dynamics simulation. *Mol. Divers.* **2021**, *25*, 1963–1977, https://doi.org/10.1007/s11030-021-10211-9.
41. Zhong, S.; Hou, Y.; Zhang, Z.; Guo, Z.; Yang, W.; Dou, G.; Lv, X.; Wang, X.; Ge, J.; Wu, B.; Pan, X.; Wang, H.; Yang, Q.; Mou, Y. Identification of novel natural inhibitors targeting AKT Serine/Threonine Kinase 1 (AKT1) by computational study. *Bioengineered* **2022**, *13*, 12003–12020, https://doi.org/10.1080/21655979.2021.2011631.
42. Nagendran, S.; Balasubramaniyan, S.; Irfan, N. Virtually screened novel sulfathiazole derivatives as a potential drug candidate for methicillin-resistant *Staphylococcus aureus* and multidrug-resistant tuberculosis. *J. Biomol. Struct. Dyn.* **2023**, *41*, 5086–5095, https://doi.org/10.1080/07391102.2022.2079002.
43. Chen, C.; Wang, T.; Wu, F.; Huang, W.; He, G.; Ouyang, L.; Xiang, M.; Peng, C.; Jiang, Q. Combining structure-based pharmacophore modeling, virtual screening, and in silico ADMET analysis to discover novel tetrahydro-quinoline based pyruvate kinase isozyme M2 activators with antitumor activity. *Drug Des. Devel. Ther.* **2014**, *8*, 1195–1210, https://doi.org/10.2147/DDDT.S62921.
44. Kotb, A.R.; Abdallah, A.E.; Elkady, H.; Eissa, I.H.; Taghour, M.S.; Bakhotmah, D.A.; Abdelghany, T.M.; El-Zahabi, M.A. Design, synthesis, anticancer evaluation, and *in silico* ADMET analysis of novel thalidomide analogs as promising immunomodulatory agents. *RSC Adv.* **2023**, *13*, 10488–10502, https://doi.org/10.1039/D3RA00066D.
45. Xu, D.; Xue, G.; Peng, B.; Feng, Z.; Lu, H.; Gong, L. High-Throughput Docking and Molecular Dynamics Simulations towards the Identification of Potential Inhibitors against Human Coagulation Factor XIIa. *Comput. Math. Methods Med.* **2020**, *2020*, 2852051, https://doi.org/10.1155/2020/2852051.
46. Xu, C.; Zhang, H.; Mu, L.; Yang, X. Artemisinins as Anticancer Drugs: Novel Therapeutic Approaches, Molecular Mechanisms, and Clinical Trials. *Front. Pharmacol.* **2020**, *11*, 529881, https://doi.org/10.3389/fphar.2020.529881.
47. Hassanzadeh, M.; Bagherzadeh, K.; Amanlou, M. A comparative study based on docking and molecular dynamics simulations over HDAC-tubulin dual inhibitors. *J. Mol. Graph. Model.* **2016**, *70*, 170–180, https://doi.org/10.1016/J.JMGM.2016.10.007.

Supplementary materials: click here